

## A Minimax Approach for Access Point Setup Optimization in IEEE 802.11n Wireless Networks

Kyaw Soe Lwin, Nobuo Funabiki, Chihiro Taniguchi, Khin Khin Zaw, Md. Selim Al Mamun,  
Minoru Kuribayashi

Department of Electrical and Communication Engineering, Okayama University  
3-1-1 Tsushimanaka, Okayama 700-8530, Japan

Wen-Chung Kao

Department of Electrical Engineering, National Taiwan Normal University  
162, Section 1, Heping E. Rd., Taipei, 106, Taiwan

Received: February 13, 2017

Revised: May 5, 2017

Accepted: May 30, 2017

Communicated by Satoshi Ohzahata

### Abstract

Recently, an IEEE 802.11n *access point (AP)* prevailed over the *wireless local area network (WLAN)* due to the high-speed data transmission using the *multiple input multiple output (MIMO)* technology. Unfortunately, the signal propagation from the 802.11n AP is not uniform in the circumferential and height directions because of the multiple antennas for MIMO. As a result, the data transmission speed between the AP and a host could be significantly affected by their relative setup conditions. In this paper, we propose a *minimax approach for optimizing the 802.11n AP setup condition* in terms of the angles and the height in an indoor environment using throughput measurements. First, we detect a bottleneck host that receives the weakest signal from the AP in the field using the *throughput estimation model*. To explore optimal values of parameters for this model, we adopt the versatile *parameter optimization tool*. Then, we optimize the AP setup by changing the angles and the height while measuring throughput. For evaluations, we verify the accuracy of the model using measurement results and confirm the throughput improvements for hosts in the field by our approach.

*Keywords:* Wireless local area network, access point setup, MIMO, throughput estimation model, parameter optimization

## 1 Introduction

Currently, *IEEE 802.11n* devices have been extensively applied in wireless local area networks (WLANs) with the strengths of higher data rates, wider coverage areas, dual band operations, and backward compatibility. The 802.11n protocol adopts several new technologies to increase the data transmission rate up to *600Mbps*, such as the *multiple input multiple output (MIMO)*, the channel bonding, and the frame aggregation. Among them, MIMO allows a single radio channel to support multiple data streams by using multiple antennas at the transmitter and the receiver [1]. Then, the antenna configuration, the mutual coupling, and the propagation environment may remarkably impact on the MIMO capacity.

The signal propagation from an IEEE 802.11n device is not uniform in the circumferential and height directions because of the multiple antennas adopted for MIMO. Thus, by changing the setup in terms of the orientation and height of the transmitting device, the receiving signal strength at the receiver could be different. In WLANs, an *access point (AP)* generally plays the transmitter role and a host (PC) does the receiver, because a conventional PC user downloads more data from the Internet. Therefore, the setup of the AP should be optimized so that the hosts in the WLAN will receive stronger signals to increase the data transmission speed.

In this paper, we propose a *minimax approach for optimizing the 802.11n AP setup condition* with regard to the orientation and the height of the AP. This approach seeks to reach the maximization of the overall throughput performance of the hosts that are covered by the AP, by finding the AP setup that can maximize the throughput of the host that suffers from the minimum throughput, called *bottleneck host*. In our approach, the bottleneck host is first found by simulations using the *throughput estimation model*. Then, the optimal AP setup condition is found by manually changing the setup while measuring the throughput between the AP and the bottleneck host. However, the alternative method does not exist to adjust the AP setup than manual operations. Thus, to reduce manual loads, the bottleneck host is found by simulations without measuring all host locations.

In our approach, the throughput estimation model for one wireless communication link consists of two steps. First, it calculates the *receiving signal strength* at the receiver using the *log-distance path loss model* [2]. Next, it calculates the *throughput* using the *sigmoid function*. To improve the estimation accuracy, which is an important factor in designing WLANs [3]-[6], the parameters in both functions are tuned by applying the *parameter optimization tool*. By comparing the throughput estimation errors between the manual tuning and the tool, the effectiveness of the tool is verified.

For evaluations, we consider three network fields of offices in two buildings in Okayama University. First, we examine the accuracy of the throughput estimation model using throughput measurement results. The same bottleneck host is found by the model and the measurements for any AP in the three fields. Then, we optimize the setup of each AP through maximizing the throughput against the bottleneck host by changing the orientation and height of the AP. The average throughput of all the hosts in each field is enhanced by up to 30%.

Conventionally, APs are allocated in the network field after surveying signal strengths at many points from APs located at several positions using related software tools. In [3], Gibney et al. presented a WLAN modeling, design and evaluation tool that can be used to automatically optimize the number of required APs and the positions to meet site-specific demands in indoor environments. In [7], Lee et al. proposed an approach of optimizing the AP placement and channel assignment in WLANs by formulating the optimal integer linear programming (ILP) problem. To improve the throughput performance, our approach could be applied to the APs allocated by these approaches.

As well, several studies have been reported for antennas and their propagation features in MIMO systems. In [8], Jensen et al. presented that antenna properties such as the radiation pattern, the polarization, the array configuration, and the mutual coupling can impact on MIMO systems. In [9], Zhu et al. introduced a robotic positioning system to automatically control the position and orientation of the antenna array. The results have confirmed that MIMO performance will be notably affected by changing the position and orientation of the antenna array. In [10], Piazza et al. introduced reconfigurable antenna array for MIMO systems. It is proved that different antenna geometry will generate different radiation patterns. In addition, they demonstrated the advantage of changing the antenna configuration based on the spatial characteristics of the MIMO channel. In [11], Forooshani et al. studied the effect of  $4 \times 4$ -ULA (uniform-linear-array) antenna configuration on MIMO-based APs in a real underground service tunnel. It is revealed that the antenna array orientation, the separation, and the polarization will crucially influence the performance of multiple-antenna systems in the underground tunnel. Moreover, our previous measurement results also show the effect of the orientation and placement height of APs on throughput in indoor environments as well as outdoor environments in [12]-[14].

The rest of this paper is organized as follows: Section 2 discusses the motivation of our approach. Section 3 presents the minimax approach for the AP setup optimization. Sections 4 and 5 display the throughput estimation model and the parameter optimization tool adopted in our approach, respectively. The evaluations are provided in Section 6. Finally, Section 7 remarks the conclusion

of this paper with future works.

## 2 Motivation

In this section, we introduce the motivation of the proposed approach through discussions of antenna radiations in MIMO.

### 2.1 Multiple Antennas in MIMO

The IEEE 802.11n protocol adopts MIMO to increase the transmission capacity. MIMO not only takes the advantage of multipath communications using multiple antennas at the transmitter and the receiver, but also enhances the performance of the wireless communication system. Due to the increasing computing power of the embedded CPU and the reducing device size, multiple antennas and complex signal processing programs could be implemented on one board. Figure 1 demonstrates the internal antenna layout of NEC WG2600HP AP [15] with four antennas for MIMO.

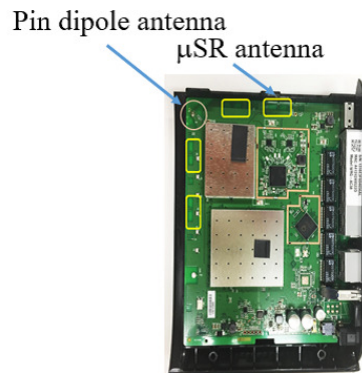


Figure 1: Internal antenna layout of NEC WG2600HP.

### 2.2 Non-symmetric Radiations in MIMO

The multiple antenna layout of a MIMO device will make a significant impact on the overall radiation pattern and strongly affect the performance of the device [10][16]. In general, an antenna could be categorized as the *omnidirectional antenna* and the *directional antenna* based on the radiation pattern. Most of APs and mobile devices deploy the omnidirectional antenna, either monopole or dipole. Figure 2 exhibits the radiation patterns of two dipole antennas that are separated by  $0.25\lambda$  at the operating frequency of  $2.45GHz$  for the MIMO system [10].

Due to the multiple antennas, the radiation pattern of the MIMO device is not symmetric in the horizontal and vertical directions, as shown in Figure 2 (a) and (b) respectively. Particularly, for the vertically polarized omnidirectional antenna, it radiates the strongest signal power in the horizontal direction, dropping to zero directly above and below the antenna [17].

### 2.3 Importance of AP Setup Optimization

In order to improve the throughput performance of WLAN, the transmitting device or AP is expected to be set up properly so that the receiving device or host will receive the strongest signal from the AP, since the radiation pattern of the MIMO device is not symmetric. Hence, the AP setup optimization in terms of the orientation and height becomes an important task to maximize the performance of

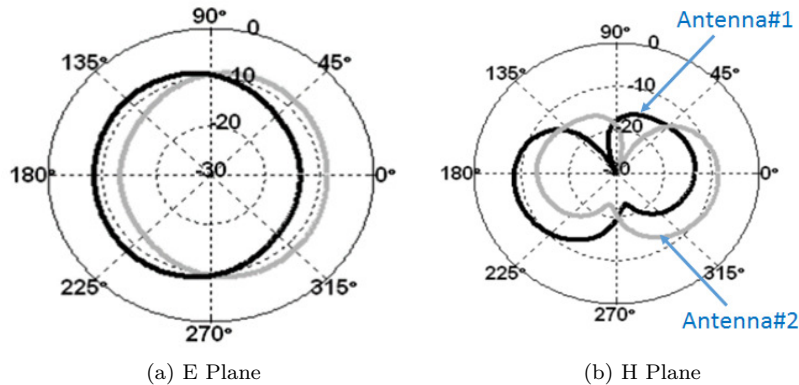


Figure 2: Radiation pattern (in dB) of two antennas at 2.4GHz.

WLAN. As well, the orientation of an AP could be changed along the three axes in Figure 3. Thus, the setup angle on each axis of the AP should be optimized for the orientation optimization.

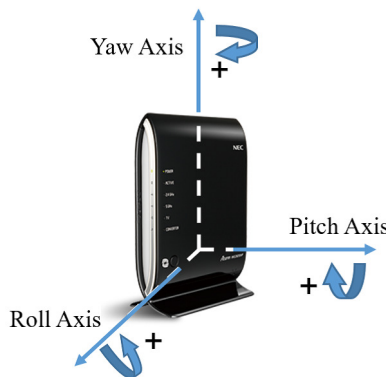


Figure 3: Three axes.

### 3 Minimax Approach for AP Setup Optimization

In this section, we present the minimax approach for the AP setup optimization in WLAN.

#### 3.1 Overview

As mentioned in the previous section, the setup of the IEEE 802.11n AP has essential effects on the performance of WLAN. To optimize the AP setup while reducing the labor cost, we propose the minimax approach for the AP setup condition optimization. In this approach, the manual setup adjustments of the AP are merely applied for the maximization of the throughput between the AP and the bottleneck host, in order to minimize the labor cost. The bottleneck host is found through simulation using the throughput estimation model. To improve the estimation accuracy, the parameters in the model should be tuned based on throughput measurement results in the target network field. To reduce the load of the parameter tuning process and obtain the superior results, the *parameter optimization tool* is used.

### 3.2 Procedure

The proposed approach consists of the following five steps:

- (1) The layout map of the target network field for WLAN is obtained, and the possible locations of the APs and the hosts are identified on the map.
- (2) The throughputs between the APs and the hosts in (1) are measured.
- (3) The parameters of the throughput estimation model are tuned by applying the parameter optimization tool with the measured data in (2).
- (4) The bottleneck host for each AP is detected using the throughput estimation model. That is, it is assumed that if a host could be associated with multiple APs in the field, it will be associated with the AP that provides the highest throughput among them in the model.
- (5) The setup of each AP is manually adjusted so that the measured throughput to the corresponding bottleneck host is maximized.

### 3.3 Justification of Minimax Approach

The aim of adopting the minimax approach is to minimize the labor cost for optimizing the AP setup in respect of the orientation and height. Currently, it is not considered to optimize the AP setup automatically or remotely using a machine for adjusting the AP setup, because it is concerned about the cost and impair the cost advantage of WLAN. Moreover, it is exceedingly difficult or impossible to install the machine in the network field due to the size/weight limitation and the power supply at the AP installation point. Thus, we consider the manual setup of an AP is the exclusive way to achieve the optimal results. Then, we manage to minimize the labor cost for this setup optimization. In this paper, it is clarified that the optimal setup of an AP for the bottleneck host will upgrade the overall throughput for the hosts in the network field that are covered by the same AP.

## 4 Throughput Estimation Model

In this section, we introduce the throughput estimation model in our approach.

### 4.1 Overview

This model estimates the throughput or transmission speed of a wireless communication link between a source node and a destination node in WLAN. First, this model estimates the receiving signal strength at the destination node using the *log-distance path loss model* by considering the distance and the obstacles between the end nodes. Next, it evaluates the throughput using the *sigmoid function* from the receiving signal strength. Each function possesses several parameters which may affect the estimation accuracy.

In both equations in the model, the specifications in a wireless communication link for the transmission rate, such as the number of streams, the channel bonding, and the frame aggregation, are considered in the parameter values. In our measurements, we used one stream, the channel bonding, and the frame aggregation. Thus, the parameter values in this paper represent a wireless link using them. To obtain the parameter values of the model and verify the effectiveness of the link with other specifications such as two streams, the measurements using the corresponding AP configuration are extremely important, which will be included in our future works.

### 4.2 Signal Strength Estimation by Log-distance Path Loss Model

The receiving signal strength of a host of the AP is calculated using the *log-distance path loss model* [2]:

$$P_d = P_1 - 10\alpha \log_{10} d - \sum_k n_k W_k \quad (1)$$

where  $P_d$  represents the received signal strength ( $dBm$ ) at the host,  $d$  does the distance (m) to the host from the AP,  $P_1$  does the received signal strength ( $dBm$ ) at the host at the  $1m$  distance from the AP when no obstacle exists between them,  $\alpha$  does the path loss exponent,  $n_k$  does the number of *type k* obstacles along the path between the AP and the host, and  $W_k$  does the signal attenuation factor ( $dBm$ ) for the *type k* obstacle. The value for  $\alpha$  strongly depends on the network environment. In [2], the proper value for  $\alpha$  has empirically been determined between 1.8 (lightly obstructed environment with corridors) and 5 (multi-floored buildings).

For the signal attenuation factor  $W_k$  of walls, the five types of obstacles are considered in this paper: the corridor wall, the partition wall, the intervening wall, the glass wall, and the elevator wall. The *corridor wall* represents the concrete wall between a room and the corridor that has the sufficient strength to improve the strength of the building itself. The *partition wall* indicates the wall without the sufficient strength and simply separates the successive rooms. The *intervening wall* signifies the concrete wall that has the sufficient strength, but does not separate closed rooms. The *glass wall* implies the wall composed of glass panels mounted in aluminum frames. The *elevator wall* represents the steel wall of the elevator.

### 4.3 Throughput Estimation from Received Signal Strength

From the received signal strength at the host, the throughput or data transmission speed from the AP to the host is calculated using the *sigmoid function*:

$$f(x) = \frac{a}{1 + e^{-\left(\frac{120+x}{c}\right)-b}} \quad (2)$$

where  $f(x)$  represents the estimated throughput (Mbps) when the received signal strength (dBm) at the host is  $x$  and  $a$ ,  $b$ ,  $c$  are constant coefficients.

The adoption of the sigmoid function for the throughput estimation is based on our measurement results. Figure 4 reveals the relationship between signal strengths and throughputs for the link between an AP and a host. The measured data were collected through experiments using NEC WG2600HP [15] for the AP, two Window PCs (JMicro JMC250 Gigabit Ethernet adapter for the server and Qualcomm Atheros AR9285 IEEE 802.11b/g/n wireless adapter) for the host, *iperf* for the throughput measurement software [18], and *Homedale* for the receiving signal strength measurement software [19], which were conducted in the indoor environment at Okayama University. The sigmoid function curve was illustrated there using  $a = 98$ ,  $b = 55$  and  $c = 8$ , which is well coincident with the measured data. The sigmoid function clearly reflects the relationship between measured signal strengths and throughputs, as in [20].

### 4.4 Multipath Consideration

The receiving signal estimation in Section 4.2 purely considers the signal along the *line of sight (LOS)* between the AP and the host. However, due to the *multipath effect*, the signal along a different path, which is diffracted on walls, may need to be considered, particularly in an indoor environment that is a conventional target for WLAN. In this paper, the signal along LOS is called the *direct signal* and the one along a different path is the *indirect signal* for convenience. The direct signal at the host becomes weak when several walls or obstacles exist along LOS. If the indirect signal passes only a few walls, the corresponding signal strength of the host becomes larger than the direct signal strength.

To consider the indirect signal to each host from any AP in the throughput estimation model, a *diffraction point* is selected for each pair of an AP and a host in the field such that it is located on the wall in the same room as the host and the signal strength of the AP is largest. When no wall or obstacle exists along the shortest path from the AP to this wall, the point that has the shortest distance from the AP is selected. However, if obstacles exist along the path, it is necessary

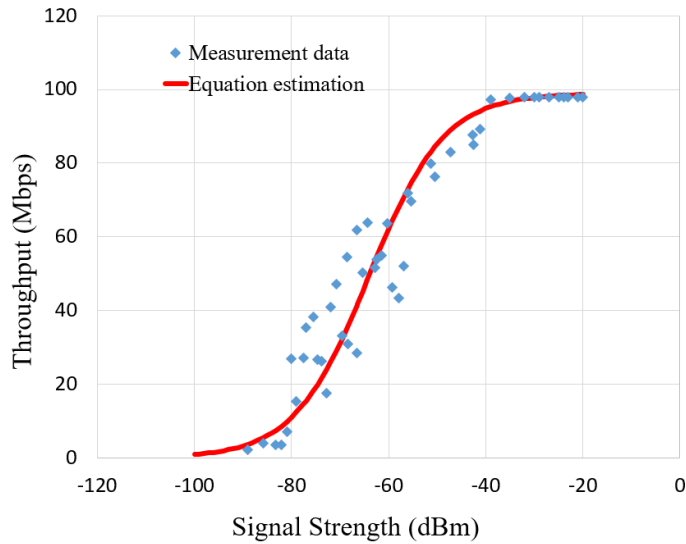


Figure 4: Sigmoid function for throughput estimation from signal strength.

to also consider another point along the wall that has the longest distance from the AP but has a less number of obstacles, which will be investigated in future studies.

Then, the indirect signal reaches the host in a straight line after this diffraction point, where the signal direction is changed and the signal strength is attenuated by the constant attenuation factor  $W_{dif}$ . Figure 5 demonstrates an example of the indirect signal through the diffraction point. It is noted that  $W_{dif}$  could be different from the direction change angle at the diffraction point, which will also be explored in future studies.

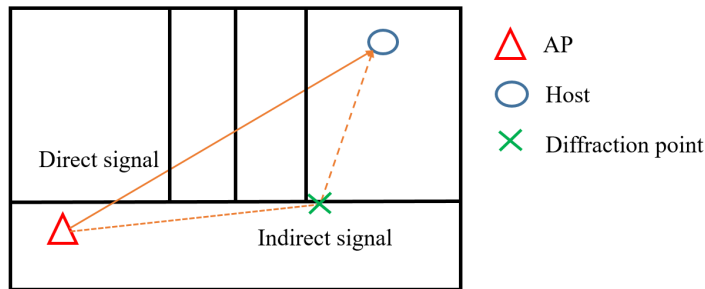


Figure 5: Example of indirect signal.

In our model, both the direct and indirect signal strengths are calculated for each pair of the AP and the host in the field. Then, if the indirect one is stronger than the direct one, the indirect signal strength will be used for the throughput estimation. In the conventional model such as the *two-ray model*, it considers the phase difference of the signals, where the receiving signal strength is obtained by summing those of the direct signal and the reflected signal from the ground (indirect signal) [21].

On the other hand, our model uses either of the direct signal or the indirect signal to estimate the receiving signal strength, not the summation of them, so that it does not need to consider the phase difference of them. In other words, the accurate calculation of the phase difference is viewed as a

challenging task in the indoor field that consists of multiple rooms since it requires a huge database of environmental characteristics and long simulation time. Therefore, our model adopts the simple approach of taking the stronger signal only, between the direct and indirect signals. The results in Table 2 and Figure 8 (c) have proved the effectiveness of our approach.

## 4.5 Procedure

The procedure of the throughput estimation model is as follows:

- (1) Calculate the Euclidean distance  $d$  (m) for each link (AP/host pair) by:

$$d = \sqrt{(AP_x - H_x)^2 + (AP_y - H_y)^2} \quad (3)$$

where  $AP_x$  and  $AP_y$  represent the  $x$  and  $y$  coordinates for the AP, and  $H_x$  and  $H_y$  represent the  $x$  and  $y$  coordinates for the host.

- (2) Identify the walls intersecting with the link. Here, the link and the wall are regarded as line segments where their intersection is judged by considering the intersection between the two line segments.
- (3) Estimate the receiving signal strength at the host using the log-distance path loss model and consider the indirect signal:

- (3-a) Calculate the receiving signal strength  $P_{dir}$  at the host through the direct signal:

$$P_{dir} = P_1 - 10\alpha \log_{10} d - \sum_k n_k W_k \quad (4)$$

where  $P_{dir}$  represents the receiving signal strength (dBm) at the host with the distance  $d$  (m) from the AP,  $P_1$  does the signal strength (dBm) of the host with 1m distance from the source node,  $\alpha$  does the distance attenuation factor that should be optimized,  $n_k$  does the number of walls with type  $k$ , and  $W_k$  does the signal attenuation factor (dBm) of the type  $k$  wall.

- (3-b) Calculate the receiving signal strength through the indirect signal:

- 1) Calculate the receiving signal strength  $P_{dif}$  (dBm) at the diffraction point for each host using (5).
- 2) Calculate the receiving signal strength  $P_{ind}$  (dBm) at the host by the indirect signal, where the receiving signal strength at 1) is used as the transmitting signal strength from the diffraction point using (6).

$$P_{dif} = P_1 - 10\alpha \log_{10} r - \sum_k n_k W_k \quad (5)$$

$$P_{ind} = P_{dif} - 10\alpha \log_{10} t - W_{dif} \quad (6)$$

where  $r$  (m) represents the distance between the AP and the diffraction point,  $t$  (m) does the distance between the diffraction point and the host, and  $W_{dif}$  (dBm) does the attenuation factor at the diffraction point. It is observed that  $P_{ind}$  does not include the attenuation factors of the walls because the diffraction point exists in the same room as the host.

- (3-c) Select the larger one between  $P_{dir}$  and  $P_{ind}$  for the receiving signal strength  $P_h$  (dBm) at the host.

- (4) Calculate the estimated throughput  $S_h$  (Mbps) using the sigmoid function in (7).

$$S_h = \frac{a}{1 + \exp\left(-\frac{(120+P_h)-b}{c}\right)} \quad (7)$$

where  $a$ ,  $b$ , and  $c$  are constant coefficients.

## 5 Parameter Optimization Tool

In this section, we offer the parameter optimization tool for the throughput estimation model. This tool is implemented using the algorithm in [22][23] in Appendix A. That is to say, it allows a developer of an algorithm/logic program, including the throughput estimation model in this paper, to use this algorithm easily by preparing the parameter specification file in Section 5.2.1, slightly modifying the program to satisfy the two conditions in Section 5.2.2, and modifying the scrip file in Section 5.2.5.

### 5.1 Overview

The parameter optimization tool is designed to be independent from the program of the throughput estimation model. It runs the model program as its child process. The effectiveness of the adopted parameter values to run the model program is evaluated by the output score for the program that is given in the output file. That is, this tool searches the parameter values that minimize the output score.

### 5.2 Required Files for Tool

A user of the tool is required to prepare the following five files.

#### 5.2.1 Parameter Specification File

The parameter specification file describes the condition how to change the value of each parameter during the search process. “parameter.csv” must be used as the file name. Each line in this file reflects the specification for one parameter, and must describe in the order of “parameter name”, “initial value”, “lower limit”, “upper limit”, and “change step”.

The following example shows the specifications for three parameters,  $x$ ,  $y$ , and  $z$ .

Example of parameter.csv.

```
01: x, 50, 0, 100, 5
02: y, -20, -50, 0, 2
03: z, 0.5, 0.0, 1.0, 0.1
```

#### 5.2.2 Model Program File

The model program file is a binary code file to run the throughput estimation model, which could be executed through the command line. Any name is possible for this file. In addition, this file must satisfy the following two conditions:

- (1) When the program is executed, it receives the path for the parameter file in the argument and applies the parameter values in the file to the model.
- (2) When the program is completed, it outputs the score as the evaluation value in the text file “result.txt”.

With (1), the model program can read the parameter values that are generated by the tool. With (2), the tool can read the score that is calculated in the model program. For example, the parameter file for the previous example with three parameters is explored when their initial ones are used.

#### 5.2.3 Sample Input Data File

The sample input data file contains the input data set to the model program such that the result of the program is evaluated and used to optimize the parameter values by the tool. To upgrade the accuracy of the obtained parameter values, multimodal sample input data sets should be collected and adopted in the tool.

### 5.2.4 Score Output File

The score output file involves the score from the model program to evaluate the current parameter values. The score is given by the difference between measured and estimated throughputs in the throughput estimation model.

### 5.2.5 Script File for Execution

The script file describes the sequence of the commands to execute the model program. The file name must be “run.sh”. This file also describes the paths to the input files for the model program. By modifying this script file, the user is able to change the name and the arguments for the model program, and may run multiple programs sequentially to obtain one score. In the following example, line 10 executes the model program, which is coded in Java, with three paths to the input files. When the model program is executed with multiple sample input data files continuously, the array to describe these files should be prepared and the loop procedure should be adopted.

Example of “run.sh”.

```
01: #!/bin/bash
02: DIR=$(cd $(dirname $0); pwd)
03: PARAMETER_FILE=$1
04: cd "$DIR"
05: #folder for sample input data files
06: INPUT_DIR="./file/3f_ap1/"
07: #measurement data file
08: MEASUREMENT_FILE="./file/evaluate/indoor_3f_ap1.csv"
09: #execute the model program
10: java -jar ThroughputEstimation.jar
    ${INPUT_DIR} ${MEASUREMENT_FILE}
    $PARAMETER_FILE
11: #move ‘‘result.txt’’ to the folder containing the parameter file
12: mv result.txt ‘dirname $PARAMETER_FILE‘
```

## 5.3 Processing Flow of Tool

The processing flow of the tool is as follows:

- (1) The parameter optimization tool ( $T$ ) generates the initial parameter file by copying the initial values in the parameter specification file.
- (2)  $T$  executes the script file using the current parameter file.
  - (2-a) The model program ( $M$ ) reads one sample input data file.
  - (2-b)  $M$  computes the algorithm/logic.
  - (2-c)  $M$  writes the score in the score output file.
- (3)  $T$  reads the score from the score output file.
- (4) When the termination condition is satisfied,  $T$  goes to (5). Otherwise,  $T$  goes to (6).
- (5)  $T$  changes the parameter file based on the algorithm in the next section, and goes to (2).
- (6)  $T$  selects the parameter values with the best score and outputs it.

## 6 Evaluations

In this section, we present evaluations of our approach in three network fields on our campus.

## 6.1 Network Fields

The three network fields in Figure 6 are considered, where the triangle represents the AP location and the circle does the host location. The diffraction point for each host is manually selected.

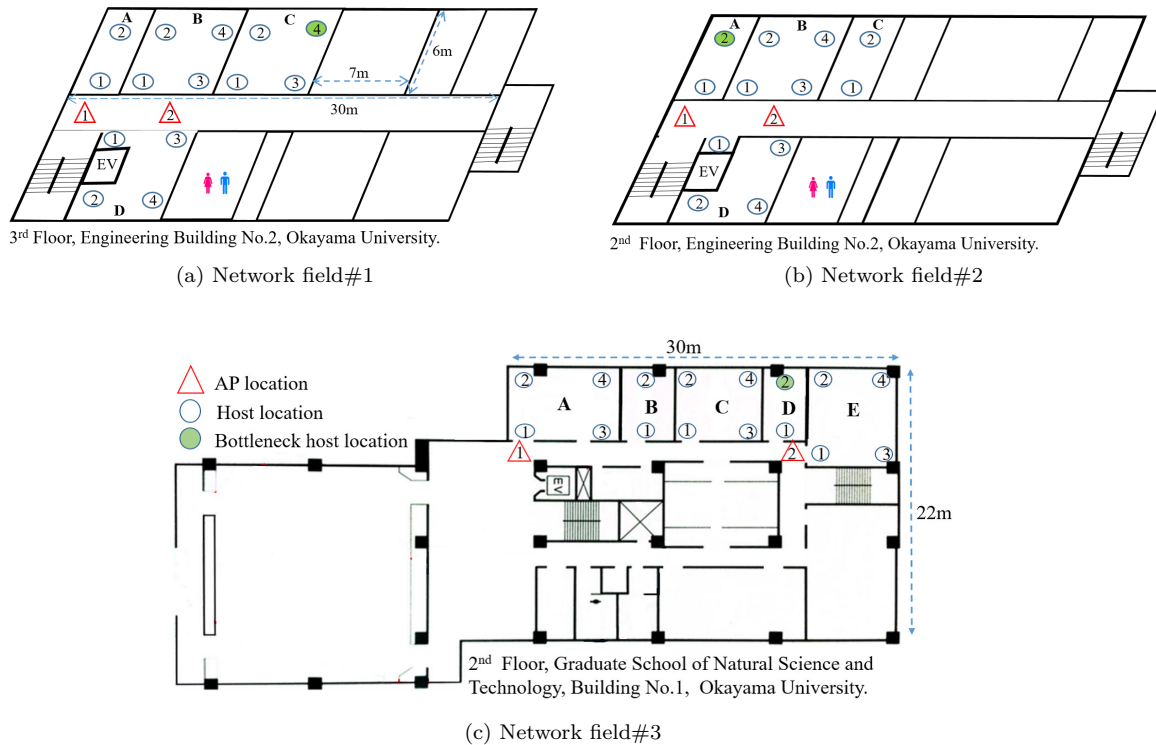


Figure 6: Three network fields.

## 6.2 Devices and Tool for Measurements

In the measurements in the three fields, one NEC WG2600HP [15] with four internal antennas for the AP and two laptop PCs with Window OS and Qualcomm Atheros AR9285 IEEE 802.11b/g/n wireless adapter for the clients are used. This AP supports the maximum transmission rate of 450Mbps (standard value) using three streams and the 40 MHz bonded channel at 2.4 GHz for IEEE 802.11n, whereas the client PC supports the maximum transmission rate of 150Mbps (standard value) with one stream only and the bonded channel. Consequently, the transmission rate for the link between the AP and the client PC in our measurements is 150Mbps. The software *iperf* is used for throughput measurements by generating TCP traffics for 50sec with 477Kbyte window size and 8Kbyte buffer size. Figure 7 illustrates this measurement setup for each link.

## 6.3 Throughput Estimation Model

First, the accuracy of the throughput estimation model, including the application of the parameter optimization tool is evaluated.

### 6.3.1 Parameter Optimization Results

First, the values of the parameters in the throughput estimation model, namely,  $P_1$ ,  $\alpha$ ,  $W_k$ , and  $W_{dif}$  in (4), (6), and (5), and  $a$ ,  $b$ , and  $c$  in (7) are optimized by applying the parameter optimization tool

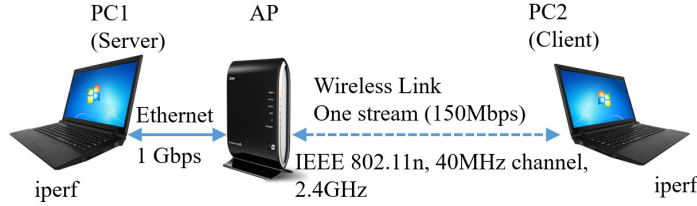


Figure 7: Measurement setup for one link.

using the measured data in the three fields.  $W_k$  is prepared for each wall type. In this paper, the corridor wall ( $k = 1$ ), the partition wall ( $k = 2$ ), the intervening wall ( $k = 3$ ), the glass wall ( $k = 4$ ), and the elevator wall ( $k = 5$ ) are examined. For the parameters in the parameter optimization algorithm,  $TB = 16$  and  $HT = 10$  are adopted. Because field#1 and field#2 are located in the same building on different floors, all the sample input data sets measured with four APs and 26 hosts in these two fields are used to select the optimal values of the parameters.

Table 1 compares the parameter values selected by manual with the direct signal only, by the tool with the direct signal only, and by the tool with the indirect signal considered. The results reveal that the value of the distance attenuation factor  $\alpha$  by the tool becomes much smaller than that by manual. By manual, the measured data sets in the open space were used, whereas by the tool, the data sets in the indoor spaces were used, which indicates that  $\alpha$  is small in indoor environments. The wall attenuation factor  $W_k$  is larger for the stronger wall.

Table 1: Parameter optimization results.

parameter	field#1,2			field#3		
	manual direct	tool direct	tool indirect	manual direct	tool direct	tool indirect
$P_1$	-20.0	-35.0	-35.0	-20.0	-37.0	-35.1
$\alpha$	3.20	2.76	2.60	3.20	2.10	2.00
$W_1$	15.0	12.9	12.5	8.0	14.3	16.4
$W_2$	6.0	3.0	3.0	3.0	2.0	3.6
$W_3$	12.0	7.0	6.5	-	-	-
$W_4$	3.0	4.0	4.0	-	-	-
$W_5$	6.0	3.9	4.0	-	-	-
$W_{dif}$	-	-	2.9	-	-	2.0
$a$	80.0	74.8	73.8	98.0	105.0	103.0
$b$	50.0	45.4	47.0	50.0	40.5	40.1
$c$	4.00	6.05	5.48	4.00	7.28	6.75

### 6.3.2 Throughput Estimation Results

Subsequently, the whole throughput estimation model is applied using the parameter values in Table 1. Table 2 summarizes the average, maximum, minimum, and standard deviation (SD) of the scores or throughput estimation errors (Mbps) on the links between the hosts and each AP in the three fields. For reference, Figure 8 displays the measured and estimated throughputs for the hosts in field#1, field#2 and field#3 respectively.

In Figure 8, the measurement throughput results are compared with three estimation results, namely *manual*, *tool (old model)*, and *tool (new model)*. In *manual*, the old model is adopted where the parameter values are tuned manually. In *tool (old model)*, the old model is adopted where the parameter values are tuned by the tool. In *tool (new model)*, the new model is adopted where the parameter values are tuned by the tool. The old model uses simply the direct signal for any link between an AP and a host to estimate the throughput. The new model selects the indirect signal if the receiving signal strength becomes stronger than that of the direct signal, to consider the *multipath effect*.

In this figure, no differences exist between *tool (old model)* and *tool (new model)* in terms of the throughput of bottleneck nodes in field#1 and field#2, because the direct signal is dominant in any link between an AP and a host including those for bottleneck nodes. This reason could originate from the fact that the number of passing walls is at most three for any link. In these fields, the tool generally improves the estimation accuracy, which confirms the effectiveness of the tool.

In field#3, the direct signal from AP1 needs to pass through five walls to reach hosts E-2 and E-4 in room E. Then, the estimated throughputs of these hosts using the direct paths in the old model become much lower than the measurement results. Consequently, E-2 is selected as the bottleneck host in *manual* and *tool (old model)*, although D-2 has been shown as bottleneck host from the measurement results.

In the new model, the indirect signal is used to estimate the throughput for hosts E-2 and E-4, where this signal passing through only one wall is diffracted at a diffraction point on the wall in room E, and the receiving signal strength is larger than that of the direct signal passing through five walls. This consideration of the indirect signal improves the throughput estimation accuracy for the two hosts, and correctly selects D-2 for the bottleneck host in field#3 by *tool (new model)*. It is critical to clarify the conditions that the new model has functioned well, which will be explored in future studies.

Table 2 indicates that the accuracy of the throughput estimations of the model is generally improved by the tool. The accuracy for the two hosts, E-2 and E-4, with AP1 in field#3, is greatly improved by considering the indirect signal. These results have verified the contributions of the parameter optimization tool and the indirect signal consideration.

However, the standard deviation of the estimation errors is increased for AP1 and AP2 in field#1 as Figure 8 shows that the errors of A-1, A-2, and D-1 for AP1 and the errors of D-1 and D-4 for AP2 are prominently increased by the model and become much larger than the errors for other hosts. From Figure 6, these hosts are located quite close to the corresponding AP, which means that the modeling for a link between an AP and its nearby host is not sufficient in the current throughput estimation model. The further improvements of the model, particularly for short links, will be studied in future works.

### 6.3.3 Bottleneck Host Detection Results

In any AP location, the bottleneck host providing the lowest measured throughput is coincident with the one found by the model. Specifically, in field#1, C-4 is the bottleneck host for AP1 and A-2 is for AP2. In field#2, C-2 is for AP1 and A-2 is for AP2. In field#3, D-2 is for AP1 and A-2 is for AP2. These outcomes support the use of the throughput estimation model to identify the bottleneck host that will be used in the following AP setup optimization.

It is assumed that only one AP has existed in the field until now, although it is more natural that two or more APs exist there. As a straightforward extension of our proposal to multiple APs, for each host, the throughput from each AP is estimated using the model, and the associated AP is selected by detecting the largest throughput. Then, the bottleneck host is selected for each AP in the field such that the estimated throughput is the smallest among the associated hosts.

However, this straightforward extension does not consider the load imbalance between the APs in the field. If the load imbalance occurs, the associated AP for a host could be different and the bottleneck host may be changed. The consideration of the load imbalance in detecting bottleneck hosts for multiple APs will be included in future studies.

Figure 9 reveals the estimated throughputs by *tool (new model)* for each host from AP1 and AP2

Table 2: Throughput estimation errors (Mbps).

AP	method	model	average	maximum	minimum	SD
field#1 AP1	manual	direct	9.42	18.7	0.62	6.46
	tool	direct	7.04	26.6	0.0	8.54
	tool	indirect	6.93	26.6	0.11	8.49
field#1 AP2	manual	direct	11.4	26.0	0.58	8.42
	tool	direct	9.29	24.6	0.1	9.06
	tool	indirect	9.11	25	0.02	9.07
field#2 AP1	manual	direct	19.1	34.6	5.07	9.95
	tool	direct	11	19	3.2	5.20
	tool	indirect	11	18.9	3.4	5.04
field#2 AP2	manual	direct	18.7	31.8	4.96	8.39
	tool	direct	8.83	15.5	1.75	4.19
	tool	indirect	8.96	15.4	2.46	4.17
field#3 AP1	manual	direct	13.2	38.2	0.83	11.16
	tool	direct	6.79	19.3	0.0	5.46
	tool	indirect	4.65	12.2	0.04	4.19
field#3 AP2	manual	direct	16.36	38.96	4.18	9.58
	tool	direct	8.57	20.91	0.05	5.80
	tool	indirect	5.29	16.14	0.01	4.77

in field#1. AP1 is selected for the associations of four hosts A-1, A-2, B-1, and D-1, whereas AP2 is selected for the other 10 hosts. That is, if the straightforward extension will be applied to this field, host A-2 is the bottleneck for AP1 and host C-4 is for AP2. The throughput of the bottleneck host for AP1 is much larger than that for AP2. Therefore, it is noticed that the consideration of the load imbalance among the two APs is critical in this field.

## 6.4 AP Setup Optimization

The AP setup is optimized by manually changing the orientation and height of the AP to increase the measured throughput between the AP and the corresponding bottleneck host. In other words, AP1 in field#1, AP2 in field#2, and AP1 in field#3 are considered in the setup optimization. The shaded circle in Figure 6 represents the corresponding bottleneck host that was found in Section 6.3.3.

### 6.4.1 Orientation Optimization

First, the orientation of the AP is optimized by rotating the AP from  $-90^\circ$  to  $+90^\circ$  with  $30^\circ$  interval along the roll and yaw axes. The pitch axis was not considered because no improvement has been observed. From the internal antenna layout of this AP in Figure 1, the change of the pitch angle is equivalent to the change of the height. During the following roll angle and yaw angle optimizations, the height of the AP was fixed at  $1.35m$  in the field#1 and field#3, and at  $0.9m$  in the field#2, as the best heights found in Section 6.4.4.

### 6.4.2 Roll Angle Optimization

Figure 10 (a) shows the throughput measurement results for different roll angles in the three fields. It indicates that  $90^\circ$  roll angle provides the highest throughput of the bottleneck host in the three fields. To elaborate, the throughput increases to  $38Mbps$  in field#1,  $37Mbps$  in field#2, and  $43Mbps$  in field#3. On the other hand,  $0^\circ$  provides the lowest throughput of  $17Mbps$  in field#1,  $-60^\circ$  does the lowest one of  $18Mbps$  in field#2, and  $-30^\circ$  does the lower one of  $19Mbps$  in field#3. The highest

throughput becomes more than twice of the lowest one. Thus, the optimization of the setup roll angle of the AP is critical for the throughput performance.

#### 6.4.3 Yaw Angle Optimization

Figure 10 (b) demonstrates the throughput measurement results for different yaw angles in the three fields. It indicates that the  $0^\circ$  yaw angle provides the highest throughput of the bottleneck host in the three fields. In details, the throughput increases to  $38Mbps$  in field#1,  $37Mbps$  in field#2, and  $43Mbps$  in field#3. On the other hand,  $90^\circ$  provides the lowest throughput of  $28Mbps$  in field#1,  $-30^\circ$  does the lowest one of  $20Mbps$  in field#2, and  $30^\circ$  provides the lowest one of  $28Mbps$  in field#3. It means the highest throughput is more than 30% higher than the lowest one. Thus, the optimization of the setup yaw angle of the AP is extremely important as well.

#### 6.4.4 Height Optimization

Next, the height of the AP is optimized by changing it from  $0m$  up to  $1.80m$  with the  $0.45m$  interval. To change the height, plastic shelves were used. It is noted that the ceiling height of the measured room is  $2.4m$ . During the height optimization, the roll/yaw angles of the AP were fixed at the best ones found in Sections 6.4.2 and 6.4.3.

Figure 11 unveils the throughput measurement results for different AP heights in the three fields. It conveys that  $1.35m$  provides the highest throughput of the bottleneck host in the field#1 and field#3, and  $0.9m$  does in field#2. Specifically, the throughput increases to  $38Mbps$  in field#1,  $37Mbps$  in field#2, and  $43Mbps$  in field#3. On the other hand,  $0m$  provides the lowest throughput of  $13Mbps$  in field#1 and of  $29Mbps$  in field#3, and  $1.8m$  does the lowest one of  $24Mbps$  in field#2. It implies the highest throughput is more than 30% higher than the lowest one. Likewise, the optimization of the setup height of the AP plays a principal role in the experiment.

#### 6.4.5 Overall Host Throughput Improvements

Finally, the overall throughput improvement among the hosts in each network field by the AP setup optimization is investigated. Figure 12 shows the throughput of each host in the three fields before and after the setup optimization. Table 3 summarizes the average throughput improvements by the proposed AP setup optimization for the six AP locations in the three network fields. These results reflect the fact that the proposed setup optimization is qualified to improve the average throughput in any field and the individual throughput for most of the hosts. Specifically, for AP1 in field#2, the average throughput is improved from  $40.48Mbps$  to  $52.88Mbps$ , which means 30.66% improvement.

Table 3: Average throughput improvements.

field	AP	before Opt. (Mbps)	after Opt. (Mbps)	improvement (%)
field#1	AP1	51.06	65.23	27.77
	AP2	57.90	67.29	16.22
field#2	AP1	40.48	52.88	30.66
	AP2	49.09	52.13	6.28
field#3	AP1	64.26	70.42	9.59
	AP2	69.55	78.63	13.05

## 7 Conclusion

This paper presented a minimax approach for the access point setup optimization in IEEE 802.11n wireless local area networks in indoor environments. The throughput estimation model with the parameter optimization tool was adopted to accurately detect the bottleneck host in the network

field. Through extensive experiments in three network fields, it was noticed that our approach has improved overall throughputs of the hosts in the field.

In future works, the throughput estimation model will be further improved for short links and in considering the indirect signal with the best diffraction point and the diffraction angle effect. The load imbalance will be considered in identifying bottleneck hosts for multiple APs in the network field. The conditions of required throughput measurements in the field will also be investigated to achieve the sufficient accuracy of the model in finding the bottleneck host. Then, the proposed approach will be applied in various network fields.

## Acknowledgments

This work is partially supported by JSPS KAKENHI (16K00127). The authors would like to thank Debnath Sumon Kumar, Kwenga Ismael, and Lee Che-Wei for their helps in throughput measurements.

## References

## References

- [1] M. S. Gast, "802.11n: a survival guide," 1st ed., O'Reilly, 2012.
- [2] D. B. Faria, "Modeling signal attenuation in IEEE 802.11 wireless LANs," Tech. Report, TR-KP06-0118, Stanford Univ., July 2005.
- [3] A. M. Gibney, M. Klepal, and D. Pesch, "A wireless local area network modeling tool for scalable indoor access point placement optimization," Proc. Spring Simulation Multiconf., Society for Computer Simulation International, pp. 163-170, Apr. 2010.
- [4] K. Farkas, Á. Huszák, and G. Gódor, "Optimization of Wi-Fi access point placement for indoor localization," *Network. Commun.*, vol. 1, no. 1, pp. 28-33, July 2013.
- [5] R. F. Safna, E. J. N. Manoshantha, S. A. T. S. Suraweera, and M. B. Dissanayake, "Optimization of wireless pathloss model JTC for access point placement in wireless local area network," Proc. RSEA 2015, pp. 235-238, 2015.
- [6] M. S. A. Mamun, M. E. Islam, N. Funabiki, M. Kuribayashi, and I-W. Lai, "An active access-point configuration algorithm for elastic wireless local-area network system using heterogeneous devices," *Int. J. Network. Comput.*, vol. 6, no. 2, pp. 395-419, July 2016.
- [7] Y. Lee, K. Kim and Y. Choi, "Optimization of AP Placement and Channel Assignment in WLAN," Proc. IEEE Conference on Local Computer Networks, pp. 831-836, Nov. 2002.
- [8] M. A. Jensen, and J. W. Wallace, "A review of antennas and propagation for MIMO wireless communications," *IEEE Trans. Antenna. Propagation*, vol. 52, no. 11, pp. 2810-2824, Nov. 2004.
- [9] W. Zhu, D. Browne, and M. Fitz, "An open access wideband multiantenna wireless testbed with remote control capability," Proc. IEEE Tridentcom, pp. 72-81, Feb. 2005.
- [10] D. Piazza, N. J. Kirsch, A. Forenza, R.W. Heath, and K. R. Dandekar, "Design and evaluation of a reconfigurable antenna array for MIMO systems," *IEEE Trans. Antenna. Propagation*, vol. 56, no. 3, pp. 869-881, March 2008.
- [11] A. E. Forooshani, C. T. Lee, and D. G. Michelson, "Effect of antenna configuration on MIMO-based access points in a short tunnel with infrastructure," *IEEE Trans. Commun.*, vol. 64, no. 5, pp. 1942-1951, May 2016.

- [12] K. S. Lwin, N. Funabiki, Md. E. Islam, C. C. Chew, and Y. Tani, "Throughput measurements in outdoor environment with different AP placement heights and orientations for IEEE 802.11n wireless networks," Proc. IEEE Hiroshima Section Student Symp., pp. 406-409, Nov. 2015.
- [13] K. S. Lwin, N. Funabiki, and Md. E. Islam, "Throughput measurements with various indoor AP placement conditions for IEEE 802.11n wireless networks," Proc. IEICE General Conf., BS-3-35, March 2016.
- [14] N. Funabiki, K. S. Lwin, M. Kuribayashi, and I. W. Lai, "Throughput measurements for access-Point installation optimization in IEEE 802.11n wireless networks," Proc. IEEE ICCE-TW, pp. 218-219, May 2016.
- [15] NEC Inc., "WG2600HP manual," <http://www.aterm.jp/support/manual/pdf/am1-002673.pdf>.
- [16] D. Kong, E. Mellions, D. Halls, A. Nix and G. Hilton, "Throughput sensitivity for antenna pattern and orientation in 802.11n networks," Proc. IEEE 22nd International Symposium on Personal, Indoor and Mobile Radio Communications, pp. 809-813, Sep. 2011.
- [17] Cisco Systems Inc., "Antenna patterns and their meaning," White Paper, 2007, [http://www.cisco.com/c/en/us/products/collateral/wireless/aironet-antennas-accessories/prod\\_white\\_paper0900aecd806a1a3e.pdf](http://www.cisco.com/c/en/us/products/collateral/wireless/aironet-antennas-accessories/prod_white_paper0900aecd806a1a3e.pdf).
- [18] ACD.net, Iperf Speed Testing, <http://support.acd.net/wiki/index.php?title=IperfSpeedTesting>.
- [19] Software Verzeichnis development. Homedale WLAN Monitor, <http://www.the-sz.com/products/homedale/>.
- [20] M. E. Islam, K. S. Lwin, M. A. Mamum, N. Funabiki, and I. W. Lai, "Measurement results of three indices for IEEE 802.11n wireless networks in outdoor environments," Proc. IEEE Hiroshima Section Student Symp., pp. 410-414, Nov. 2015.
- [21] R. Akl, D. Tummala, and L. Xinrong, "Indoor propagation modeling at 2.4 GHz for IEEE 802.11 networks," Proc. Sixth IASTED Int. Multi-Conf. Wireless. Optical Commun., July 2006.
- [22] T. Sekioka, N. Funabiki, and T. Higashino, "A proposal of an improved function synthesis algorithm using genetic programming," IEICE Trans. D1, vol. J83-D-I, no.4, pp.407-417, April 2000.
- [23] T. Sekioka, Y. Yokogawa, N. Funabiki, T. Higashino, T. Yamada, and E. Mori, "A proposal of a lip contour approximation method using the function synthesis," IEICE Trans. D2, vol. J84-D-II, no.3, pp.459-470, March 2001.

## Appendix

### A Parameter Optimization Algorithm

In this section, we show the parameter optimization algorithm adopted in the *parameter optimization tool*.

#### A.1 Symbols in Algorithm

The following symbols are used in the algorithm:

- $P$ : the set of the  $n$  parameters for the algorithm/logic in the model program whose values should be optimized.

- $p_i$ : the  $i$ th parameter in  $P$  ( $1 \leq i \leq n$ ).
- $\Delta p_i$ : the change step for  $p_i$ .
- $t_i$ : the tabu period for  $p_i$  in the tabu table.
- $S(P)$ : the score of the algorithm/logic using  $P$ .
- $P_{best}$ : the best set of the parameters.
- $S(P_{best})$ : the score of the algorithm/logic where  $P_{best}$  is used.
- $L$ : the log or cache of generated parameter values and their scores.

## A.2 Algorithm Procedure

The algorithm procedure that minimizes the score is described as follows:

- (1) Clear the generated parameter log  $L$ .
- (2) Set the initial value in the parameter file for any  $p_i$  in  $P$ , and set 0 for any tabu period  $t_i$ , and set a large value for  $S(P_{best})$ .
- (3) Generate the neighborhood parameter value sets for  $P$  by:
  - (3-a) Randomly select one parameter  $p_i$  for  $t_i = 0$ .
  - (3-b) Calculate parameter values of  $p_i^-$  and  $p_i^+$  by:

$$p_i^- = p_i - \Delta p_i, \text{ if } p_i > \text{lower limit,}$$

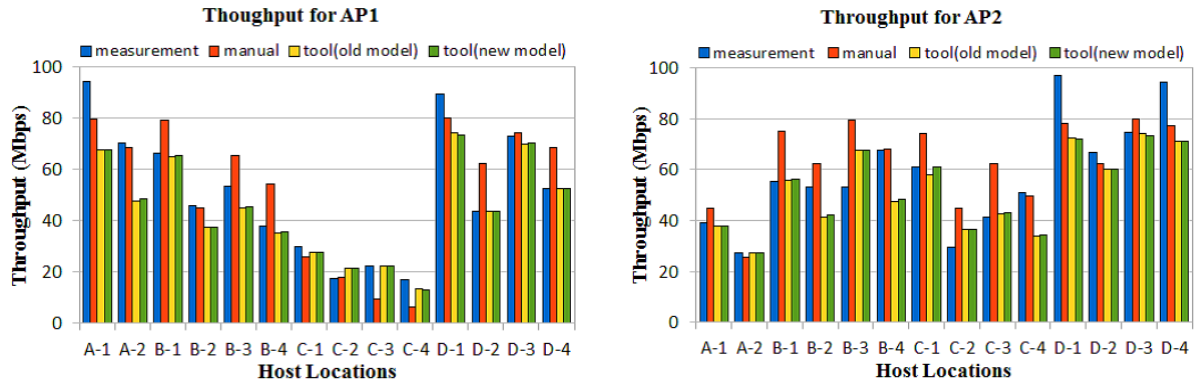
$$p_i^+ = p_i + \Delta p_i, \text{ if } p_i < \text{upper limit.}$$

- (3-c) Generate the neighborhood parameter value sets  $P^-$  and  $P^+$  by replacing  $p_i$  by  $p_i^-$  or  $p_i^+$ :

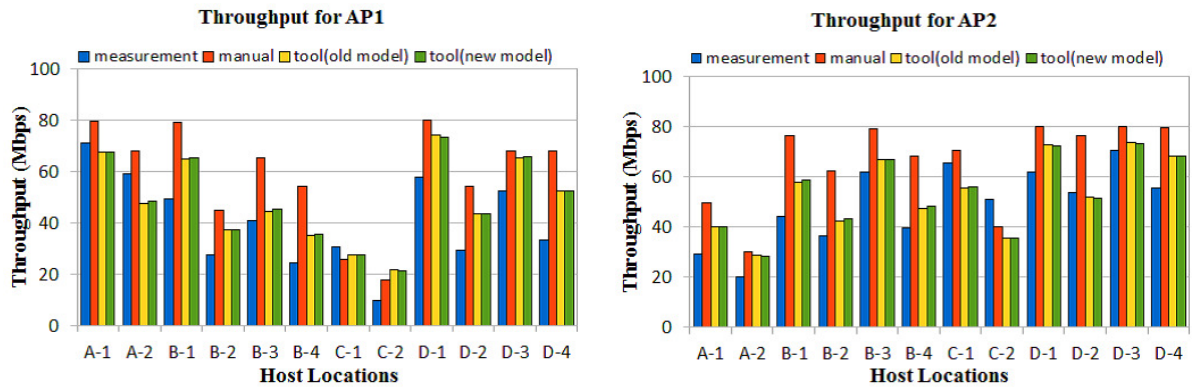
$$P^- = \{p_1, p_2, \dots, p_i^-, \dots, p_n\}$$

$$P^+ = \{p_1, p_2, \dots, p_i^+, \dots, p_n\}$$

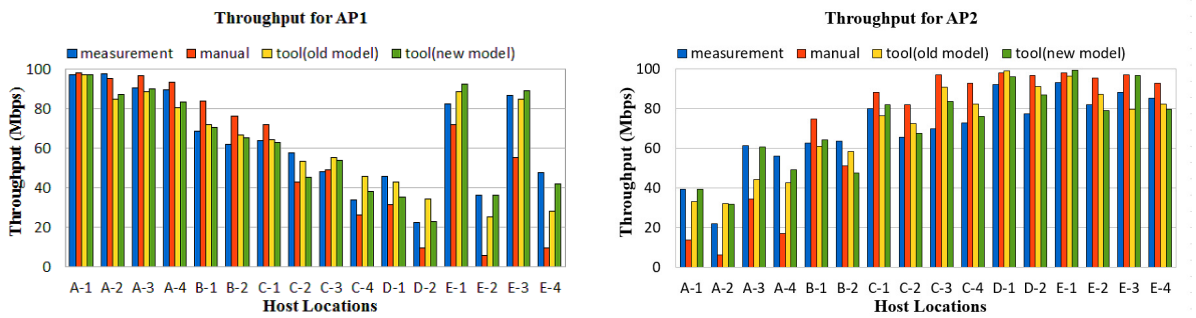
- (4) When  $P$  ( $P^-, P^+$ ) exists in  $L$ , obtain  $S(P)$  ( $S(P^-)$ ,  $S(P^+)$ ) from  $L$ . Otherwise, execute the model program using  $P$  ( $P^-, P^+$ ) to obtain  $S(P)$  ( $S(P^-)$ ,  $S(P^+)$ ), and write  $P$  and  $S(P)$  ( $P^-$  and  $S(P^-)$ ,  $P^+$  and  $S(P^+)$ ) into  $L$ .
- (5) Compare  $S(P)$ ,  $S(P^-)$ , and  $S(P^+)$ , and select the parameter value set that has the largest one among them.
- (6) Update the tabu period by:
  - (6-a) Decrement  $t_i$  by  $-1$  if  $t_i > 0$ .
  - (6-b) Set the given constant tabu period  $TB$  for  $t_i$  if  $S(P)$  is largest at (5) and  $p_i$  is selected at (3-a).
- (7) When  $S(P)$  is continuously largest at (5) for the given constant times, go to (8). Otherwise, go to (3).
- (8) When the hill-climbing procedure in (9) is applied to the given constant times  $HT$ , terminate the algorithm and output  $P_{best}$ . Otherwise, go to (9).
- (9) Apply the hill-climbing procedure:
  - (9-a) If  $S(P) < S(P_{best})$ , update  $P_{best}$  and  $S(P_{best})$  by  $P$  and  $S(P)$ .
  - (9-a) Reset  $P$  by  $P_{best}$ .
  - (9-c) Randomly select  $p_i$  in  $P$ , and randomly change the value of  $p_i$  within its range.
  - (9-d) Go to (3).



(a) Throughput results in field#1



(b) Throughput results in field#2



(c) Throughput results in field#3

Figure 8: Measured and estimated throughput results.

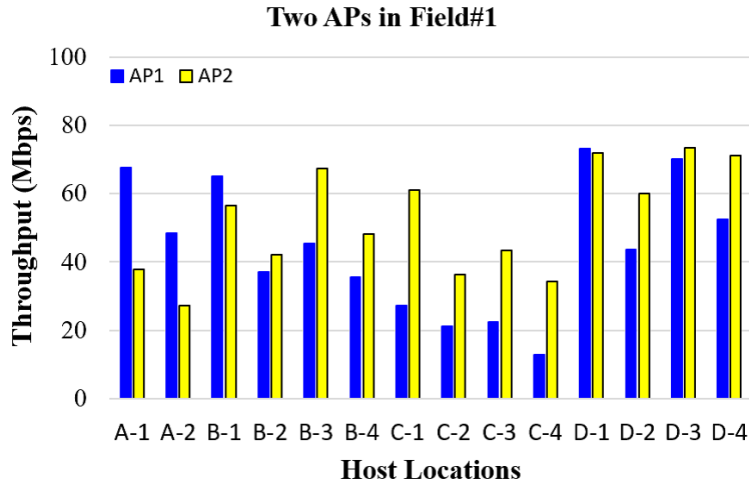


Figure 9: Throughputs for two APs in field#1.

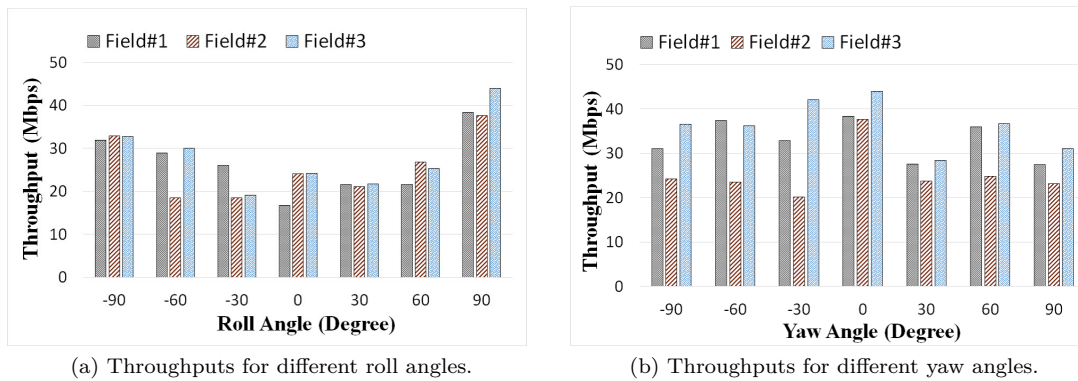


Figure 10: Bottleneck host throughputs for different orientations.

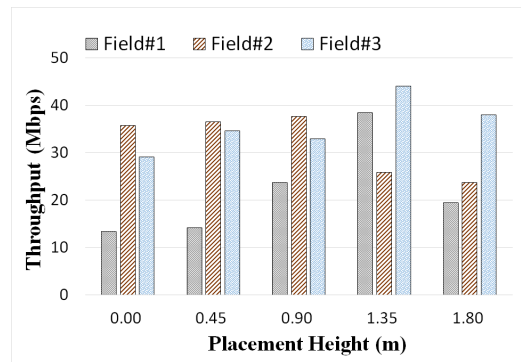
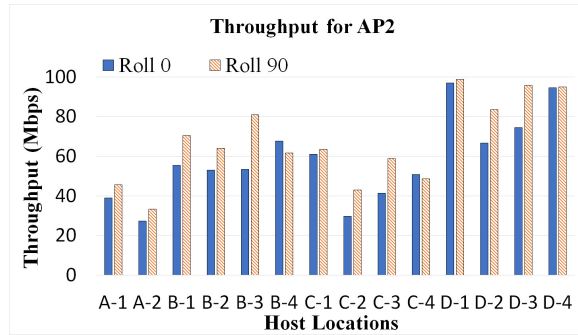
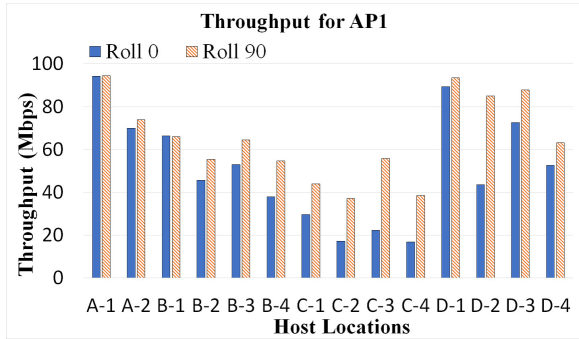
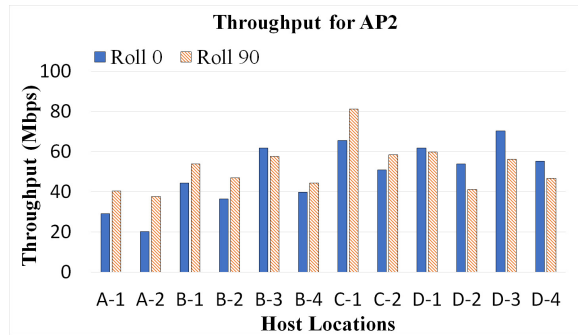
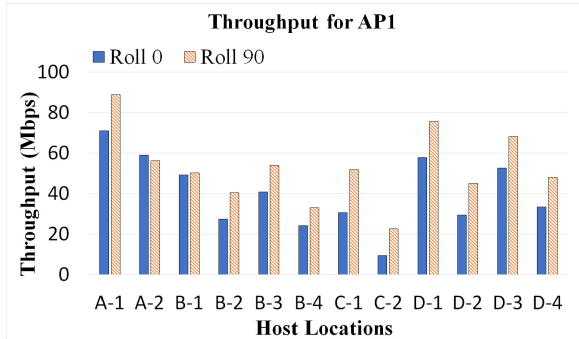


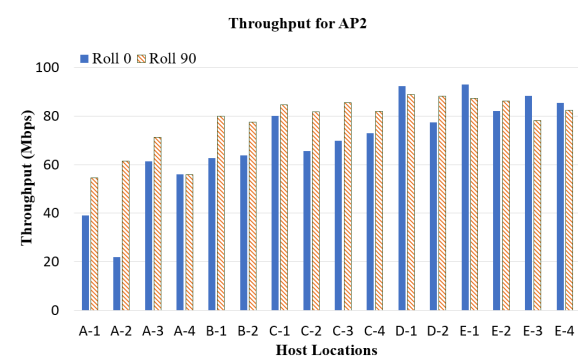
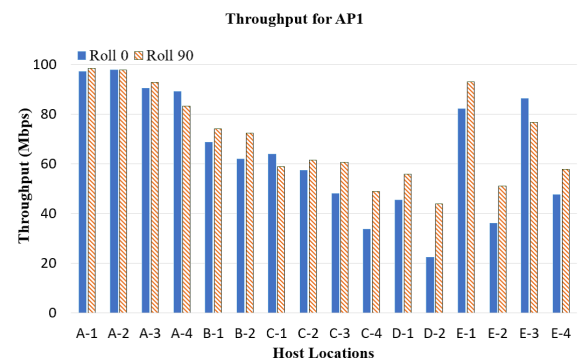
Figure 11: Bottleneck host throughputs for different heights.



(a) Network field#1



(b) Network field#2



(c) Network field#3

Figure 12: Throughput improvements by setup optimizations.